

## Anisotropic Interference of Three-Wave and Double Two-Wave Frequency Mixing in GaAs†

Eli Yablonovitch, C. Flytzanis, and N. Bloembergen

*Gordon McKay Laboratory, Harvard University, Cambridge, Massachusetts 02138*

(Received 5 July 1972)

It is shown that two-step, two-wave mixing makes a substantial contribution to the total three-wave mixing process in a noncentrosymmetric crystal. The efficiency of generating  $2\omega_1 - \omega_2$  was observed as a function of the difference frequency  $\omega_1 - \omega_2$ , the electric polarization vector, and the propagation direction. This method allowed the determination of the *true* third-order susceptibility  $\chi^{(3)}$ , in both sign and magnitude, in terms of  $[\chi^{(2)}]^2$ .

The frequency combination  $\omega_3 = 2\omega_1 - \omega_2$  is interesting for nonlinear optics because it permits the observation of third-order mixing under phase-matched conditions.<sup>1</sup> In a crystal of NaCl structure, the frequency  $2\omega_1 - \omega_2$  can only be generated by the electronic third-order nonlinearity  $\chi^{(3)}$ . In the diamond structure, however, the Raman nonlinearity may also contribute. As a first step, the incident waves at  $\omega_1$  and  $\omega_2$  drive the optical phonon mode at  $\omega_1 - \omega_2$ . This beats in the second step, again with the wave at  $\omega_1$ , to create the output frequency  $2\omega_1 - \omega_2$ . An interference between the Raman nonlinearity, which is resonant when  $\omega_1 - \omega_2 = \omega_T$ , and the nonresonant electronic nonlinearity  $\chi^{(3)}$  has been observed in diamond.<sup>2</sup>

For crystals in the zinc-blende structure, e.g., GaAs, additional contributions to the three-wave mixing  $2\omega_1 - \omega_2$  must be considered. Because of the lack of inversion symmetry the Raman modes are simultaneously infrared active. The Raman contribution will therefore split into two, with a resonance at both the transverse and longitudinal optical phonon frequencies.<sup>3</sup> The lack of inversion symmetry also implies that second-order optical mixing is allowed. An electromagnetic wave at the second harmonic  $2\omega_1$  can be generated, and it may beat again with  $\omega_2$  to produce a polarization at  $2\omega_1 - \omega_2$ . Additionally, second-order mixing can generate a polariton wave at  $\omega_1 - \omega_2$  which may mix again with  $\omega_1$  to produce  $2\omega_1 - \omega_2$ . This last process has previously been used to observe the polariton momentum-matching condition.<sup>4</sup>

In this experiment we have observed for the first time the interference between the direct three-wave mixing and the various two-step processes which were described above. This allowed us to measure the *true* third-order electronic susceptibility  $\chi^{(3)}$  in terms of  $[\chi^{(2)}]^2$ , where  $\chi^{(2)}$  is the second-order electronic susceptibility. Fur-

ther, it allowed us to extract the true value of the anisotropy of the electronic susceptibility  $\chi^{(3)}$  in GaAs. We anticipate that this quantity is of fundamental importance since it directly probes the anisotropy of the electronic valence distribution in these crystals.

Experiments were carried out in single crystals of high-resistivity GaAs. The nonlinearity of conduction electrons could be ignored.<sup>5</sup> Two synchronized pulsed CO<sub>2</sub> lasers were used to provide two linearly polarized waves at a number of frequency pairs  $\omega_1$  and  $\omega_2$ . The experimental setup is shown in Fig. 1. The frequencies  $\omega_1$ ,  $\omega_2$ , and  $\omega_3$  all lie in the transparent region of the crystal, while the frequency  $\Delta\omega = \omega_1 - \omega_2$  was made to ap-

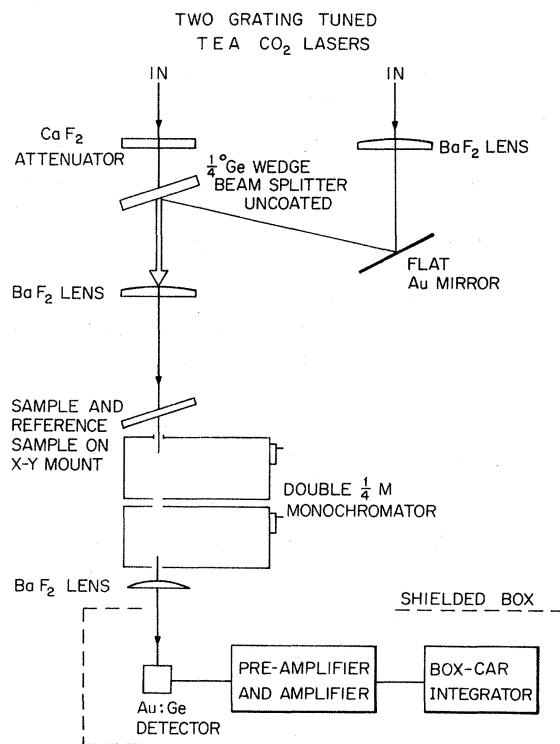


FIG. 1. The experimental configuration.

proach the optical phonon frequency  $\omega_T$  from below. The efficiency of generating  $\omega_3$  was observed as a function of the directions of polarization and propagation of the waves at  $\omega_1$  and  $\omega_2$ . This made possible the separation of the direct contribution  $\chi^{(3)}$  from the two-step processes  $\tilde{\chi}^{(3)}$ . The apparent observed nonlinear susceptibility is  $\chi_{\text{obs}}^{(3)} = \chi^{(3)} + \tilde{\chi}^{(3)}$ .

Before presenting the general theoretical expressions, three especially simple geometries will be considered first to illustrate the basic physical ideas.

(1) The electric fields at  $\omega_1$  and  $\omega_2$  are parallel to the cubic [100] direction. Only the  $xyz$  component of the Raman and second-order optical susceptibility tensors is nonvanishing in  $\bar{4}3m$  symmetry. Therefore, two-step processes are absent in this geometry and  $\omega_3$  can only be created by the direct third-order nonlinearity  $\chi_{xxxx}^{(3)}(\omega_1, \omega_1, -\omega_2)$ . Since the coherence length  $\pi/(2k_1 - k_2 - k_3)$  is very long, the mixing process can be quite efficient.

(2) The electric fields at  $\omega_1$  and  $\omega_2$  are polarized along [110], while the waves propagate along the [001] direction. Symmetry permits the creation of a second-order nonlinear electric polarization and vibration only in the longitudinal

direction [001]. No intermediate transverse electromagnetic or polariton waves are excited. There are, however, two-step contributions from longitudinal excitations. An intermediate longitudinal optical phonon wave at  $\omega_1 - \omega_2$  will be generated and will result in a Raman contribution which is resonant at  $\omega_L$ . In addition, there will be a longitudinal electric fields at both  $\omega_1 - \omega_2$  and at  $2\omega_1$ . The last contribution is given by

$$E_z(2\omega_1) = \frac{-4\pi P^{(2)}(2\omega_1)}{\epsilon(2\omega_1)} \exp(2i\vec{k}_1 \cdot \vec{r}). \quad (1)$$

All these intermediate excitations, when beating again with the incident fields in the second step, will interfere with the direct third-order contribution  $\frac{1}{2}\chi_{xxxx}^{(3)} + \frac{3}{2}\chi_{xyxy}^{(3)}$ .

(3) The electric fields at  $\omega_1$  and  $\omega_2$  are again polarized along [110], but the waves now propagate along the face diagonal [110]. In this case, symmetry decrees that the second-order nonlinear electric polarization  $P^{(2)}$  will be in the transverse direction [001]. The accompanying transverse optical phonon wave will produce a Raman contribution. In addition a transverse second-harmonic wave and a polariton wave will be generated. The second-harmonic wave, for example, can be written as a sum of a driven and a free wave<sup>6</sup>:

$$E(2\omega_1) = \frac{4\pi P^{(2)}(2\omega_1)}{\epsilon(2\omega_1) - \epsilon(\omega_1)} \{ \exp[i2\vec{k}_1 \cdot \vec{r}] - \exp[i\vec{k}(2\omega_1) \cdot \vec{r}] \}, \quad (2)$$

where  $\vec{k}(2\omega_1)$  is the propagation vector of the free wave. In the second step of the two-step process, the field in (2) will beat against the incident wave at  $\omega_2$  to produce a third-order polarization at  $2\omega_1 - \omega_2$ . The free-wave part of (2) together with the incident wave will be phase mismatched, and the corresponding two-step contribution will be negligible in our geometry, where all the  $\vec{k}$ 's are parallel. The phase-matched situation is equivalent to polariton resonance, as discussed elsewhere.<sup>4,7</sup>

When, however, the driven part of (2) beats against the incident wave, then a polarization with a propagation vector  $2\vec{k}_1 - \vec{k}_2$  will be produced, i.e., with the same propagation vector as in the direct three-wave mixing, and accordingly phase matched. Therefore, the second step of the two-step process is always able to take full advantage of the phase matching of the direct process, even though each step is individually badly mismatched. The same reasoning applies to the phase-mismatched intermediate polariton wave.

The total contribution to the three-wave mixing can be obtained by carrying to third order the iterative solution of the following three equations: the equation of motion of the phonon coordinate  $Q$ ,

$$M(\ddot{Q} + \Gamma\dot{Q} + \omega_T^2 Q) = e^* E + \frac{1}{2}\alpha_T EE; \quad (3)$$

the definition of the electric polarization,

$$P = Ne^* Q + \chi^{(1)} E + N\alpha_T EQ + \chi^{(2)} EE + \chi^{(3)} EEE; \quad (4)$$

and Maxwell's equation,

$$\nabla^2 E - \nabla(\nabla \cdot \vec{E}) - \frac{1}{c^2} \frac{\partial^2 E}{\partial t^2} = \frac{4\pi}{c^2} \frac{\partial^2 P}{\partial t^2}, \quad (5)$$

where the vector subscripts have been suppressed;  $\alpha_T = \partial\alpha/\partial Q$  is the Raman coefficient,  $M$  the reduced ionic mass,  $\Gamma$  the damping rate,  $N$  the molecular density,  $e^*$  the effective charge, and  $\chi^{(i)}$  the pure electronic  $i$ th-order susceptibility.

The two-step contribution  $\tilde{\chi}^{(3)}$  to the three-wave mixing can be written

$$\tilde{\chi}_{ijmn}^{(3)}(\omega_1, \omega_1, -\omega_2) = \sum_{l,p} (A_{ijl} A_{lmn} - B_{ini}' B_{ljm}' + B_{inl} \hat{k}_i \hat{k}_p B_{pjm} - A_{ijl}' \hat{k}_l \hat{k}_p A_{pnm}'),$$

where  $\hat{k}$  is the unit vector in the propagation direction, and only the  $xyz$  components of the tensors  $A$ ,  $A'$ ,  $B$ , and  $B'$  are nonvanishing. They are given by

$$A_{xyz}^2 = U \left( \frac{N\alpha_L^2}{MD(\omega_L)} - \frac{N\alpha_T^2}{MD(\omega_T)} - \frac{16\pi[\chi^{(2)}]^2}{\epsilon_\infty} \right) + \frac{N\alpha_T^2}{MD(\omega_T)}, \quad A_{xyz}'^2 = (U-1) \left( \frac{N\alpha_L^2}{MD(\omega_L)} - \frac{N\alpha_T^2}{MD(\omega_T)} - \frac{16\pi[\chi^{(2)}]^2}{\epsilon_\infty} \right),$$

$$B_{xyz}^2 = V(8\pi/\epsilon_\infty)[\chi^{(2)}]^2, \quad B_{xyz}'^2 = (V-1)(8\pi/\epsilon_\infty)[\chi^{(2)}]^2,$$

where

$$\alpha_L = \alpha_T \left( 1 - \frac{\epsilon_0 - \epsilon_\infty}{\epsilon_\infty C} \right), \quad C = \frac{Ne^* \alpha_T}{2M\omega_T^2 \chi^{(2)}}, \quad U = \frac{\epsilon(\Delta\omega)}{\epsilon(\Delta\omega) - \epsilon_\infty}, \quad V = \frac{\epsilon(2\omega_1)}{\epsilon(2\omega_1) - \epsilon(\omega_1)},$$

$$D(\omega) = \omega^2 - (\omega_1 - \omega_2)^2 - i\Gamma(\omega_1 - \omega_2).$$

Here  $\epsilon_0$  and  $\epsilon_\infty$  are the low- and high-frequency dielectric constants, respectively, and  $\epsilon(\Delta\omega)$  is the dielectric constant at  $\Delta\omega$  from which the polariton dispersion curve can be derived. The two-step contribution  $\chi^{(3)}$  depends on  $\chi^{(2)}$  and  $\alpha_T$ , both of which have been measured absolutely in GaAs.<sup>8</sup> Therefore, by determining the relative magnitude of the direct and the two-step contribution, it is possible to calibrate the absolute value of the third-order susceptibility.

In our experimental conditions,  $V$  (which is related to the coherence length for second-harmonic generation) was an order of magnitude larger than  $U$  (which is related to the coherence length for polariton generation). Therefore, the tensors  $B$  and  $B'$  were much larger than  $A$  and  $A'$ . Consequently, our absolute calibration was sensitive only to  $\chi^{(2)}$ , the second-harmonic generation coefficient, and to the coherence length for second-harmonic generation.

The coherence length<sup>9</sup> is thought to be known to 2%; therefore, the main uncertainty<sup>10,11</sup> is in  $\chi^{(2)}$ . We have used  $\chi^{(2)} = 2.7 \times 10^{-7}$  esu. By measuring the relative efficiency of  $2\omega_1 - \omega_2$  mixing for various geometries, we obtain, for the purely electronic third-order nonlinear susceptibilities

$$\chi_{xyxy}^{(3)} = (70 \pm 10\%) [\chi_{xyz}^{(2)}]^2 = 0.51 \times 10^{-11} \text{ esu},$$

$$\delta = \chi_{xyxy}^{(3)} / \chi_{xxxx}^{(3)} = 0.53 \pm 10\%,$$

$$\chi_{xxxx}^{(3)} = 0.97 \times 10^{-11} \text{ esu}.$$

For comparison we give our measured  $\delta$  in germanium,<sup>12</sup> where the two-step contribution is absent:

$$\delta_{Ge} = 0.52 \pm 2\%.$$

We see that the ratio  $\delta$  has the same value in GaAs as in Ge. This resolves the paradoxical difference<sup>13</sup> in sign of the anisotropy  $\sigma = 1 - 3\delta$  for these two compounds, which had been reported<sup>5</sup> before the two-step contributions were recog-

nized. Since the ratio  $\delta$  reflects the band anisotropy, it would be interesting to see if this value is a universal property of all covalent crystals in the zinc-blende and diamond structure.

In conclusion, we have shown that the double two-wave mixing process via nonresonant, non-phase-matched electronic second-harmonic generation can make a substantial contribution to the three-wave mixing. The interference of this contribution with the true third-order susceptibility permits us to extract the magnitude and anisotropy for the latter in GaAs. Substantial indirect contributions of comparable relative magnitude are expected to occur in many other III-V and II-VI compounds on the basis of standard (anharmonic oscillator) models for the nonlinearities. The relative importance depends on the numerical values of the nonresonant  $\chi^{(2)}$  and  $\chi^{(3)}$  and on the degree of momentum mismatch for second-harmonic generation in each substance. We would emphasize here the importance of including two-step processes whenever third-order nonlinear optical effects are studied in noncentrosymmetric crystals. For example, there will exist two-step contributions in the Franz-Keldysh effect<sup>14</sup> and in two-photon absorption<sup>15</sup> experiments.

†Work supported by the Joint Services Electronics Program under Contract No. N00014-67-A-0298-0006.

<sup>1</sup>P. D. Maker and R. W. Terhune, Phys. Rev. **137**, A801 (1965).

<sup>2</sup>M. D. Levenson, C. Flytzanis, and N. Bloembergen, to be published.

<sup>3</sup>C. Flytzanis, Phys. Rev. B **6**, 1264 (1972).

<sup>4</sup>J. P. Coffinet and F. DeMartini, Phys. Rev. Lett. **22**, 60 (1969).

<sup>5</sup>J. J. Wynne, Phys. Rev. **178**, 1295 (1968).

<sup>6</sup>N. Bloembergen, *Nonlinear Optics* (Benjamin, New York, 1965).

<sup>7</sup>J. Gelbwachs, R. H. Pantell, H. E. Puthoff, and J. M. Yarborough, Appl. Phys. Lett. **14**, 258 (1969); C. H.

Henry and C. G. B. Garrett, *Phys. Rev.* **171**, 1058 (1968).

<sup>8</sup>W. D. Johnston and I. P. Kaminow, *Phys. Rev.* **188**, 1209 (1969).

<sup>9</sup>Unpublished index of refraction data of G. D. Boyd were used. See in addition, G. D. Boyd, F. R. Nash, and D. F. Nelson, *Phys. Rev. Lett.* **24**, 1298 (1970); C. J. Johnson, G. H. Sherman, and R. Weil, *Appl. Opt.* **8**, 1667 (1969).

<sup>10</sup>J. H. McFee, G. D. Boyd, and P. H. Schmidt, *Appl.*

*Phys. Lett.* **17**, 57 (1970).

<sup>11</sup>B. F. Levine and C. G. Bethea, *Appl. Phys. Lett.* **20**, 272 (1972).

<sup>12</sup>Our measurement agrees with the work of C. C. Wang and N. W. Ressler, *Phys. Rev.* **132**, 1827 (1970).

<sup>13</sup>C. Flytzanis, *Phys. Lett.* **31A**, 273 (1970).

<sup>14</sup>D. E. Aspnes, *Phys. Rev. Lett.* **26**, 1429 (1971).

<sup>15</sup>D. C. Hauessen and H. Mahr, *Phys. Rev. Lett.* **26**, 838 (1971); D. Fröhlich, E. Mohler, and P. Wiesner, *ibid.* **26**, 554 (1971).

## Electronic Density of States at Transition-Metal Surfaces

R. Haydock, Volker Heine, M. J. Kelly, and J. B. Pendry  
*Cavendish Laboratory, Cambridge, England*

(Received 7 August 1972)

A completely real-space solution of the tight-binding Hamiltonian has allowed a realistic interpretation of ion-neutralization spectroscopy and some ultraviolet photoelectron spectroscopy data in terms of the surface density of states at transition-metal surfaces. The rms width of the  $d$ -band density of states decreases as the square root of the coordination number of surface atoms. The extent to which this is observed depends on the surface sensitivity of the experimental technique.

Recent experimental results of Eastman,<sup>1</sup> using ultraviolet photoelectron spectroscopic techniques (UPS), show that with increasing energy of the incident photon the rms width of the optical density of states in Ni narrows from  $\sim 2.5$  eV for 21.2-eV photons to  $\sim 2.0$  eV for 40.8-eV photons. Measurements on Cr and Cu, but only for lower incident photon energy, show a similar but less marked narrowing for Cr, but no narrowing for Cu. Published data for ion neutralization spectroscopy (INS) from Ni and Cu surfaces<sup>2</sup> show a surface  $d$ -band density of states consistent with the same overall width as the bulk bands<sup>3</sup> but having a single central peak and smaller rms width [Fig. 1]. All these observations seem to us to be explicable in terms of the surface sensitivity of the experimental technique, and, in the case of INS results, can be compared with calculations performed to establish the effect of the surface environment on the density of states. By the latter we mean the local<sup>4</sup> density of states at the surface  $\mathcal{N}_s(E)$ , namely, the density of levels  $\mathcal{N}(E)$  weighted by the probability density  $|\psi|^2$  of the states of energy  $E$  at a surface atom.

The main qualitative effect, namely, the reduction in the rms width of the density of states at the surface, can be understood simply in two ways. Firstly, for tight-binding bands Cyrot-Lackmann<sup>5,6</sup> has shown that the second moment  $\mu_2$  of  $\mathcal{N}_s(E)$  [or of  $\mathcal{N}(E)$  in the bulk] is proportional to the number of nearest neighbors  $z$ . This is rigorously

true for a tight-binding band of  $s$  states and approximately so for  $d$  bands. Thus the rms width varies as  $\sqrt{z}$ , where  $z=7, 8, 9$  for (110), (100), and (111) surfaces on face-centered cubic metals, compared with  $z=12$  in the bulk. Secondly we have the behavior of  $\mathcal{N}_s(E)$  at the band maximum

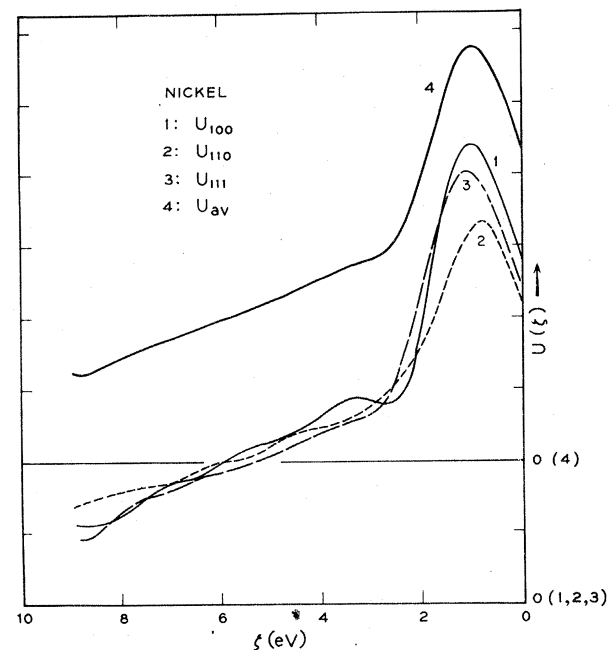


FIG. 1. The density of states, as measured by INS, at the three principal surfaces of Ni from experimental results of Hagstrum.